

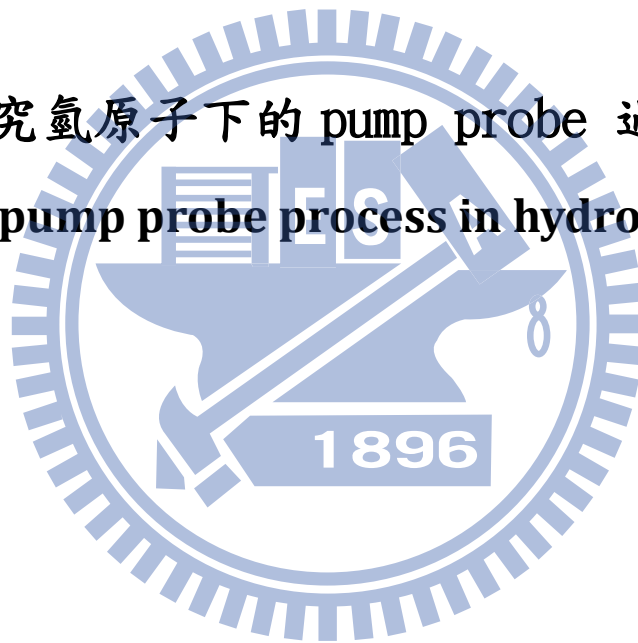
國立交通大學

物理研究所

碩士論文

研究氫原子下的 pump probe 過程

Study of pump probe process in hydrogen atom



研究生：鄭玉書

指導教授：江進福 教授

中華民國九十九年七月

研究氫原子下的 pump probe 過程

Study of pump probe process in hydrogen atom

研究生：鄭玉書

Student : Yu-Shu Cheng

指導教授：江進福 教授

Advisor : Tsin-Fu Jiang



July 2010

Hsinchu, Taiwan, Republic of China

中華民國九十九年七月

研究氫原子下的 pump probe 過程

研究生：鄭玉書

指導教授：江進福

國立交通大學物理研究所碩士班

摘要

本篇論文研究以時間延遲的雷射脈衝研究電子波包。通過紅外雷射游離激發態，脈衝雷射產生激發態和的電子波包，且在延遲下產生新的連續的電子波包。從這二個步驟，分析分析波包的干涉，反映角度解析的光電子光譜。使用分析表示，來探索信息的可能性關於雷射脈衝所引起的電子波包。



Study of pump probe process in hydrogen atom

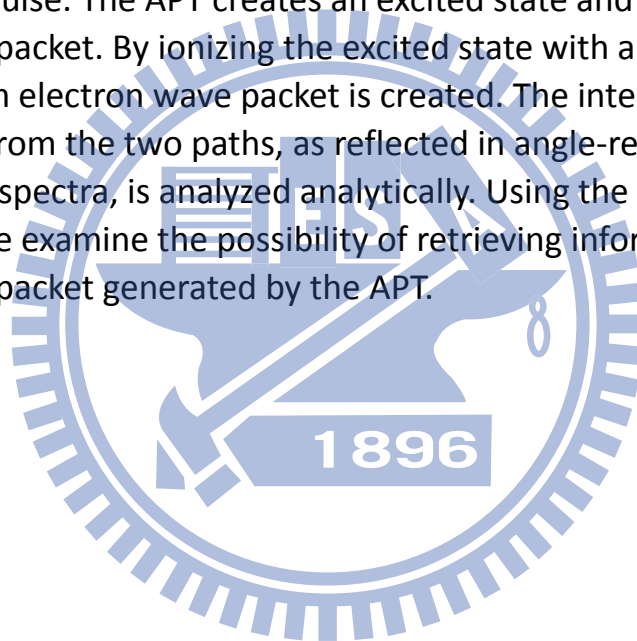
Student : Yu-Shu Cheng

Advisor : Tsin-Fu Jiang

**Institute of Physics
National Chiao Tung University**

Abstract

This thesis studies theoretically the electron wave packet generated by an attosecond pulse train (APT) which is then probed with a time-delayed laser pulse. The APT creates an excited state and a continuum electron wave packet. By ionizing the excited state with an IR, a delayed new continuum electron wave packet is created. The interference of the wave packets from the two paths, as reflected in angle-resolved photoelectron spectra, is analyzed analytically. Using the analytical expressions, we examine the possibility of retrieving information on the electron wave packet generated by the APT.



誌 謝

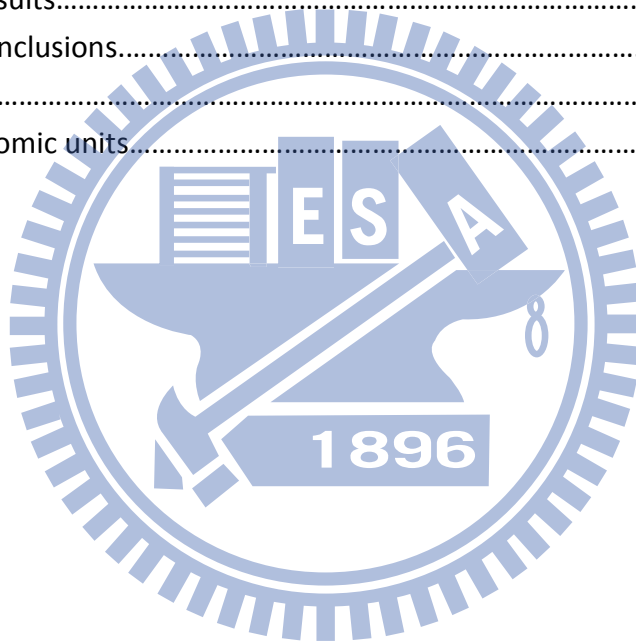
首先我要先感謝我的指導教授江進福教授，在平常從老師的身上看到老師對研究專注的態度和熱誠，在學習研究上給予我許多建議及指導。另外特別感謝李漢傑博士，在我有疑問時肯耐心地花時間指導我和幫助我。也感研究室的鄭世達學長、張繼允學長在這過程的陪伴，還有研究室同學吳明軒，一起討論、分享和許多意見交換。

也感謝壘球隊的伙伴，除了體諒我無法一起練球外也仍然給予我鼓勵，還有教會親朋好友為了我的課業研究關心和代禱，最後要感謝我的家人與女朋友的信任、肯定及支持與輔助，真是無比的感謝。



Index

摘要.....	I
Abstract.....	II
誌謝.....	III
Index.....	IV
Index of figure.....	V
Chapter 1. Introduction.....	1
Chapter 2. Two-path interference model.....	2
Chapter 3. Simpler models for the calculation of transition amplitudes.....	8
Chapter 4. Numerov method.....	10
Chapter 5. First order time-depended perturbation to continuum.....	14
Chapter 6. Results.....	20
Chapter 7. Conclusions.....	24
References.....	25
Appendix : Atomic units.....	26



Index of Figure

Figure 2-1	Pump-probe process.....	2
Figure 2-2	Single attosecond pulse (SAP).....	3
Figure 3-1	Two-- state population 3fs FWHM and 2.5 TW/cm ²	6
Figure 3-2	Two --state population 3fs FWHM and 2.5 TW/cm ²	7
Figure 4-1	Numerov method in 1ev l=0.....	12
Figure 4-2	Numerov method in 5ev l=0.....	13
Figure 5-1	$M_{p,i}^{(X)}$ amplitudes in 3fs FWHM and 75TW/cm ²	16
Figure 5-2	$M_{p,i}^{(X)}$ probability density in 3fs FWHM and 75TW/cm ²	16
Figure 5-3	$M_{p,2p}^{(L)}$ amplitudes in 3fs FWHM and 55TW/cm ²	18
Figure 5-4	$M_{p,2p}^{(L)}$ probability density in 3fs FWHM and 55TW/cm ²	19
Figure 6-1	$ M_{pi}(\tau) ^2$ in time-delay $\tau = \frac{\tau_L}{2} + \frac{\tau_x}{2}$	20
Figure 6-2	$ M_{pi}(\tau) ^2$ in time-delay $\tau = \frac{\tau_L}{2} + \frac{\tau_x}{2} + 1$	21
Figure 6-3	Angular distribution of photoelectron.....	22
Figure 6-4	Interferogram dependence of on time-delay.....	23
Figure 6-5	Interferogram for fix time-delay.....	23

1. INTRODUCTION

Attosecond pulse trains (APT) in the extreme ultraviolet (XUV) region have been produced in the process of high-order harmonic generation (HHG) by exposing rare gas atoms to intense femtosecond infrared (IR) laser pulses. These APT's can span a broad spectrum of harmonics, each with a relatively narrow bandwidth, and in the time domain, a series of attosecond bursts of radiation. Thus APT is suitable for initiating a dynamical atomic or molecular system which evolves nontrivially in time, while retaining spectral sensitivity. To probe such a wave packet in the laboratory, the most accessible tools are IR pulses that were employed to generate the APT, or the second or third harmonics of the IR. Such experiments have the advantage that the time delay between the APT and the IR can be controlled with high precision—at the level of attoseconds. Attoseconds is also the time scale needed in order to probe the electron wave packet dynamics generated by the APT.

The technology for producing APT or single attosecond pulses (SAP) is still in its infancy. Thus today only a handful of laboratories are capable of performing APT+IR or SAP+IR experiments. Ideally, the goal of a pump-probe experiment is to unravel the dynamic system after the pump. Since the dynamic system evolves in time, the probe pulse has to be applied at different delay times. While it may be of interest to observe how the results of the probe change with time delay, a more interesting and challenging question is how to retrieve information on the dynamic system from such pump-probe measurements.

2. Two-path interference model

By exposing a hydrogen atom to such an APT, the 2p state will be populated prominently among the excited states. In the meantime, the H atom can be ionized to the continuum directly. Clearly the efficiency of populating the 1s2p state and the width of the photoelectrons depend on the pulse duration of the APT.

After the pulse is over, another laser will be applied to the target again. Using laser the 2p state can be ionized by two-photon absorption to interfere with the wave packet generated directly, then a single-photon absorption will reach the same energy region.

The electron spectra are expected to show interference due to the two paths taken for the electron to reach the same kinetic energy after the probe. Here develop pump-probe model below where the time-delay dependence is given analytically.

For clarity, we define $t=0$ to be at the center of the APT pulse. The time difference between the APT and the IR is defined as the time delay, τ . The various parameters of the APT and the IR are clearly defined in Fig. 2-1, about pulse defined in Fig. 2-2

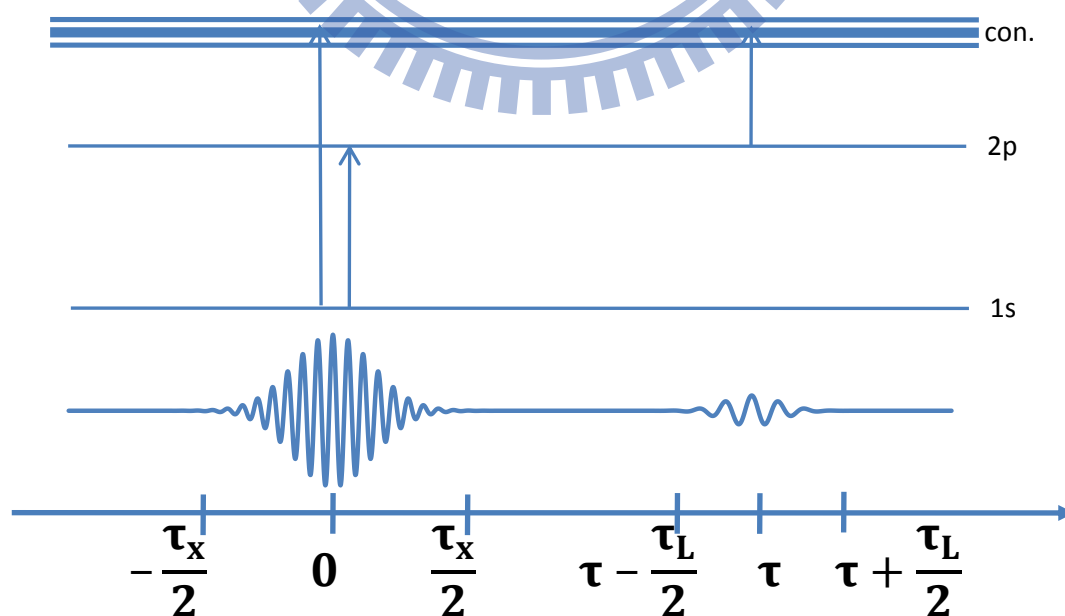


Fig.2-1. Pump-probe process

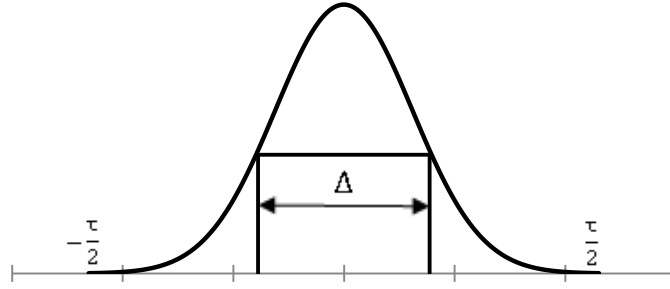


Fig.2-2. Single attosecond pulse (SAP)
 Δ = Full-Width-Half-Maximum (FWHM)

pulse duration $\tau = 2.57757\Delta\sqrt{n}$

$n=4\sim 6$ here always use $n=6$

time range = $[-\frac{\tau}{2}, \frac{\tau}{2}]$

$$H(t) = H_0 + zE_x(t) + zE_L(t - \tau)$$

Consider the time evolution operator for the whole pump-probe cycle, we can write the total evolution operator as

$$U_{\text{total}} = U(\tau + \frac{\tau_L}{2}, \tau - \frac{\tau_L}{2}) U(\tau - \frac{\tau_L}{2}, \frac{\tau_x}{2}) U(\frac{\tau_x}{2}, -\frac{\tau_x}{2})$$

For convenience, we define the propagators

$$U_x \equiv U(\frac{\tau_x}{2}, -\frac{\tau_x}{2} ; E_x(t)) \quad \tau_x = 2.57757\Delta\sqrt{n}$$

$$U_L \equiv U(\tau + \frac{\tau_L}{2}, \tau - \frac{\tau_L}{2} ; E_L(t - \tau)) \quad \tau_L = 2.57757\Delta\sqrt{n}$$

(2.1)

Such that

$$U_{\text{total}} = U_L e^{-(\tau - \frac{\tau_L}{2} - \frac{\tau_x}{2})H_0} U_x \quad (2.2)$$

Here H_0 is the field-free Hamiltonian and $e^{-(\tau - \frac{\tau_L}{2} - \frac{\tau_x}{2})H_0}$ is represented in terms of bound and continuum eigenstates $|n\rangle$ and eigenenergies ϵ_n of H_0 :

$$e^{-(\tau - \frac{\tau_L}{2} - \frac{\tau_x}{2})H_0} = \sum_n |n\rangle e^{-(\tau - \frac{\tau_L}{2} - \frac{\tau_x}{2})\epsilon_n} \langle n| \quad (2.3)$$

Substituting this into (2.2), we can write the probability amplitude as a function of the time-delay τ for transition from initial bound state $|i\rangle$ to an ionized state with photoelectron momentum \mathbf{p} as

$$M_{\mathbf{p}i}(\tau) = \sum_n e^{-i\left(\tau - \frac{t_L}{2} - \frac{t_X}{2}\right)\epsilon_n} M_{\mathbf{p}n}^{(L)} M_{ni}^{(X)} \quad (2.4)$$

where $M_{ni}^{(X)}$ and $M_{\mathbf{p}n}^{(L)}$ are probability amplitudes for transitions induced by XUV and IR pulses, respectively,

$$\begin{aligned} M_{ni}^{(X)} &= \langle n | U_X | i \rangle \\ M_{\mathbf{p}n}^{(L)} &= \langle \mathbf{p} | U_L | n \rangle \end{aligned} \quad (2.5)$$

Note that $|\mathbf{p}\rangle$ is not a plane wave but a scattering wave which is an eigenstate of H_0 with incoming boundary conditions. From the expression (2.4) we can interpret the ionization process under the pump-probe as a coherent sum of paths represented by the intermediate states n .

Note that $M_{ni}^{(X)}$ and $M_{\mathbf{p}n}^{(L)}$ are independent of the delay-time τ . Once they are obtained, then we can generate the pump-probe interferogram $|M_{\mathbf{p}i}(\tau)|^2$ as a function of τ for a given momentum \mathbf{p} by using (2.4).

For hydrogen atom in the ground state exposed to the APT introduced previously, the transition amplitude $M_{ni}^{(X)}$ for bound states other than $n=2p$ is negligible. Thus $M_{\mathbf{p}i}(\tau)$ can be approximately written as

$$M_{\mathbf{p}i}(\tau) = e^{-i\left(\tau - \frac{t_L}{2} - \frac{t_X}{2}\right)\epsilon_{2p}} M_{\mathbf{p},2p}^{(L)} M_{2p,i}^{(X)} + \sum_{\mathbf{p}'} e^{-i\left(\tau - \frac{t_L}{2} - \frac{t_X}{2}\right)\epsilon_{\mathbf{p}'}} M_{\mathbf{p}\mathbf{p}'}^{(L)} M_{\mathbf{p}'i}^{(X)} \quad (2.6)$$

where the second term on right-hand side represents the contribution from the intermediate scattering states $|\mathbf{p}'\rangle$. Since energy and momentum of a free electron are not changed by a laser field, the IR introduces a Volkov phase only.

Thus

$$M_{\mathbf{p}\mathbf{p}'}^{(L)} \approx \delta(\mathbf{p} - \mathbf{p}') \exp \left[-\frac{i}{2} \int_{-\frac{\tau}{2}}^{\frac{\tau}{2}} (\mathbf{p} + \mathbf{A}(t))^2 dt \right] \quad (2.7)$$

where $\mathbf{E}_L(t) = -\frac{d\mathbf{A}(t)}{dt}$ and \mathbf{A} is the vector potential describing the IR laser pulse.

Using this approximation, $M_{\mathbf{p}\mathbf{i}}$ can be written as a coherent sum of contributions from the two paths,

$$M_{\mathbf{p}\mathbf{i}}(\tau) = e^{-i\left(\tau - \frac{\tau_L}{2} - \frac{\tau_X}{2}\right)\epsilon_{2p}} M_{\mathbf{p},2p}^{(L)} M_{2p,\mathbf{i}}^{(X)} + e^{-i\left(\tau - \frac{\tau_L}{2} - \frac{\tau_X}{2}\right)\epsilon_p} e^{-i(\tau_L \epsilon_p + \alpha \cdot \mathbf{p} + \beta)} M_{\mathbf{p},\mathbf{i}}^{(X)} \quad (2.8)$$

where

$$\alpha = \int_{-\frac{\tau}{2}}^{\frac{\tau}{2}} \mathbf{A}(t) dt \quad \text{and} \quad \beta = \int_{-\frac{\tau}{2}}^{\frac{\tau}{2}} A^2(t) dt \quad (2.9)$$

Here the transition amplitudes $M_{\mathbf{p},2p}^{(L)}$, $M_{2p,\mathbf{i}}^{(X)}$, and $M_{\mathbf{p},\mathbf{i}}^{(X)}$ can be respectively obtained, for example, by solving the corresponding time-dependent Schrödinger equations. Introducing their magnitudes and phases such that

$$M_{\mathbf{p},\mathbf{i}}^{(X)} = a_p e^{i\phi_p}, \quad M_{2p,\mathbf{i}}^{(X)} = a_{2p} e^{i\phi_{2p}}, \quad \text{and} \quad M_{\mathbf{p},2p}^{(L)} = b_{\mathbf{p},2p} e^{i\phi_{\mathbf{p},2p}}, \quad (2.10)$$

the ionization probability density is expressed as

$$|M_{\mathbf{p}\mathbf{i}}(\tau)|^2 = a_p^2 + a_{2p}^2 b_{\mathbf{p},2p}^2 + 2a_p a_{2p} b_{\mathbf{p},2p} \cos[\Phi_{\mathbf{p},2p} - (\epsilon_p - \epsilon_{2p})\tau] \quad (2.11)$$

with

$$\Phi_{\mathbf{p},2p} = \phi_p - (\epsilon_p \tau_L + \alpha \cdot \mathbf{p} + \beta) - (\phi_{2p} + \phi_{\mathbf{p},2p}) + (\epsilon_p - \epsilon_{2p}) \left(\frac{\tau_L}{2} + \frac{\tau_X}{2} \right) \quad (2.12)$$

Note that the sinusoidal τ -dependence of $|M_{\mathbf{p}\mathbf{i}}(\tau)|^2$ is explicitly shown in (2.11).

3. Simpler models for the calculation of transition amplitudes

In the previous subsection, the effect of the pump beam is obtained by solving the time-dependent Schrödinger equation (TDSE) with a model potential for hydrogen. Since the XUV pump is not exactly in the strong field regime, it is preferable that the scattering amplitudes from the pump pulse be solved using perturbation theory. However, the pump laser is nearly resonant with the 1s to 2p transition, the scattering amplitude $M_{2p,i}^{(X)}$ can't be solved by first-order perturbation theory. Instead, we solve it by the coupled channel method. Starting with the time-dependent Schrödinger equation (TDSE),

$$i \frac{d\Psi}{dt} = [H_0 + \hat{\epsilon} \cdot \vec{r} E_X(t)] \Psi(t) \quad (3.1)$$

expand,

$$\Psi(t) = a(t)e^{-i\epsilon_{1s}t}\phi_{1s}(r) + b(t)e^{-i\epsilon_{2p}t}\phi_{2p}(r) \quad (3.2)$$

where the transition amplitude $M_{2p,i}^{(X)} \equiv a_{2p} e^{i\phi_{2p}} = b\left(\frac{\tau_X}{2}\right)$.

The two-state coupled equations can be solved numerically. Solve detail by :

$$\begin{aligned} i \frac{da}{dt} &= E(t)b(t)e^{-i(\epsilon_{2p}-\epsilon_{1s})t} \langle 1s | \hat{\epsilon} \cdot \vec{r} | 2p \rangle \\ i \frac{db}{dt} &= E(t)a(t)e^{+i(\epsilon_{2p}-\epsilon_{1s})t} \langle 2p | \hat{\epsilon} \cdot \vec{r} | 1s \rangle \end{aligned} \quad (3.3)$$

For linearly polarized light $\hat{\epsilon} = \epsilon_0$

$$\hat{\epsilon} \cdot \vec{r} = \epsilon_0 \sqrt{\frac{4\pi}{3}} Y_1^0(\vec{r}) \cdot r \quad (3.4)$$

$$E(t) = E_m \cdot f(t) \cdot \cos(\omega t + \varphi) \quad (3.5)$$

$f(t)$ = envelope, here always use gaussian = $e^{-\frac{2\ln 2}{\Delta^2}t^2}$

ω = the carrier frequency

φ = the carrier envelope phase (CEP)

Δ = FWHM

$$\begin{cases} a_r + ia_i \\ b_r + ib_i \end{cases} \quad \varphi = 0 \quad (3.6)$$

$$\Rightarrow \begin{cases} i(\dot{a}_r + i\dot{a}_i) = E_m \cdot f(t) \cdot \cos(\omega t) [b_r + ib_i] e^{-i(\epsilon_{2p} - \epsilon_{1s})t} \langle 1s | \hat{\epsilon} \cdot \vec{r} | 2p \rangle \\ i(\dot{b}_r + ib_i) = E_m \cdot f(t) \cdot \cos(\omega t) [a_r + ia_i] e^{+i(\epsilon_{2p} - \epsilon_{1s})t} \langle 2p | \hat{\epsilon} \cdot \vec{r} | 1s \rangle \end{cases} \quad (3.7)$$

$$\Rightarrow \begin{cases} i(\dot{a}_r + i\dot{a}_i) = E_m \cdot f(t) \cdot \frac{(e^{i\omega t} + e^{-i\omega t})}{2} [b_r + ib_i] e^{-i(\epsilon_{2p} - \epsilon_{1s})t} \langle 1s | \hat{\epsilon} \cdot \vec{r} | 2p \rangle \\ i(\dot{b}_r + ib_i) = E_m \cdot f(t) \cdot \frac{(e^{i\omega t} + e^{-i\omega t})}{2} [a_r + ia_i] e^{+i(\epsilon_{2p} - \epsilon_{1s})t} \langle 2p | \hat{\epsilon} \cdot \vec{r} | 1s \rangle \end{cases} \quad (3.8)$$

$\omega - (\epsilon_{2p} - \epsilon_{1s}) \approx 0$: slowly varying in time

$\omega + (\epsilon_{2p} - \epsilon_{1s}) \approx 2\omega$: fast charge in time

With Rotating wave approximation (RWA)

drop the fast oscillating term keep the slowly varying term.

$$\Rightarrow \begin{cases} i(\dot{a}_r + i\dot{a}_i) \approx \frac{E_m}{2} \cdot f(t) (b_r + ib_i) e^{+i[\omega - (\epsilon_{2p} - \epsilon_{1s})]t} \langle 1s | \hat{\epsilon} \cdot \vec{r} | 2p \rangle \\ i(\dot{b}_r + ib_i) \approx \frac{E_m}{2} \cdot f(t) (a_r + ia_i) e^{-i[\omega - (\epsilon_{2p} - \epsilon_{1s})]t} \langle 2p | \hat{\epsilon} \cdot \vec{r} | 1s \rangle \end{cases} \quad (3.9)$$

$$\omega_{21} \equiv \epsilon_{2p} - \epsilon_{1s} \quad \Delta\omega \equiv \omega - \omega_{21} = \omega - (\epsilon_{2p} - \epsilon_{1s}) \quad (3.10)$$

$$\Rightarrow \begin{cases} i(\dot{a}_r + i\dot{a}_i) \approx \frac{E_m}{2} \cdot f(t) (b_r + ib_i) (\cos \Delta\omega t + i \sin \Delta\omega t) \langle 1s | \hat{\epsilon} \cdot \vec{r} | 2p \rangle \\ i(\dot{b}_r + ib_i) \approx \frac{E_m}{2} \cdot f(t) (a_r + ia_i) (\cos \Delta\omega t - i \sin \Delta\omega t) \langle 2p | \hat{\epsilon} \cdot \vec{r} | 1s \rangle \end{cases} \quad (3.11)$$

$$\Rightarrow \begin{cases} \dot{a}_r + i\dot{a}_i \approx \frac{E_m}{2} \cdot f(t) (-ib_r + b_i) (\cos \Delta\omega t + i \sin \Delta\omega t) \langle 1s | \hat{\epsilon} \cdot \vec{r} | 2p \rangle \\ \dot{b}_r + ib_i \approx \frac{E_m}{2} \cdot f(t) (-ia_r + a_i) (\cos \Delta\omega t - i \sin \Delta\omega t) \langle 2p | \hat{\epsilon} \cdot \vec{r} | 1s \rangle \end{cases} \quad (3.12)$$

$$\Rightarrow \begin{cases} \dot{a}_r = \frac{E_m}{2} \cdot f(t) \cdot (b_r \sin \Delta\omega t + b_i \cos \Delta\omega t) \\ \dot{a}_i = \frac{E_m}{2} \cdot f(t) \cdot (-b_r \cos \Delta\omega t + b_i \sin \Delta\omega t) \\ \dot{b}_r = \frac{E_m}{2} \cdot f(t) \cdot (-a_r \sin \Delta\omega t + a_i \cos \Delta\omega t) \\ \dot{b}_i = \frac{E_m}{2} \cdot f(t) \cdot (-a_r \cos \Delta\omega t - a_i \sin \Delta\omega t) \end{cases} \quad (3.13)$$

$$\text{assume} \begin{cases} \dot{a}_r(-\infty) = 1 \\ \dot{a}_i(-\infty) = 0 \\ \dot{b}_r(-\infty) = 0 \\ \dot{b}_i(-\infty) = 0 \end{cases} \quad (3.14)$$

$$M_{2p,i}^{(X)} \equiv a_{2p} e^{i\phi_{2p}} = b\left(\frac{\tau_X}{2}\right) \quad (3.15)$$

Two-state population history of hydrogen ground state to 2p state in Fig. 3-1 and Fig. 3-2

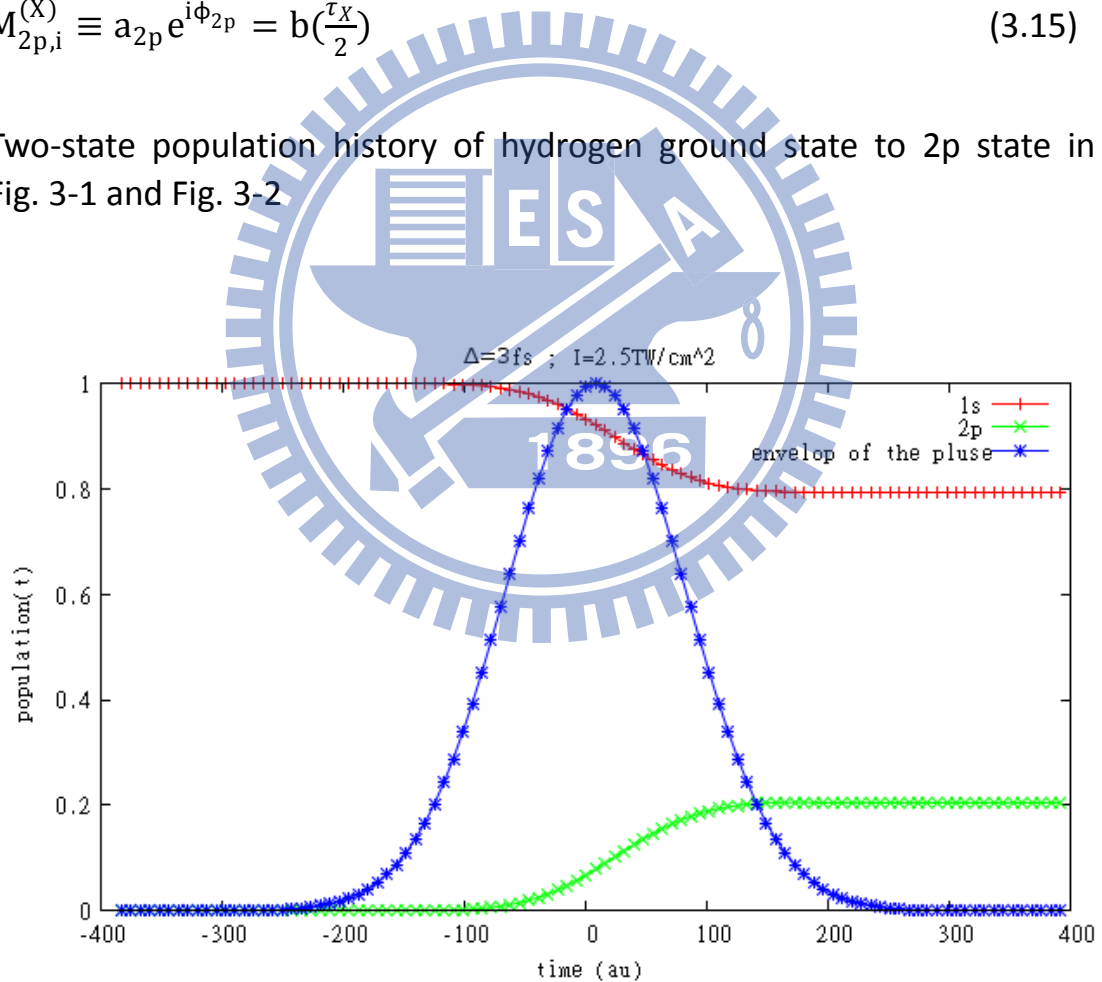


Fig.3-1. The red bar line is hydrogen ground state population history , the green cross line is 2p state population history ,and the blue star line is envelop of the pulse in 3fs FWHM and 2.5 TW/cm²

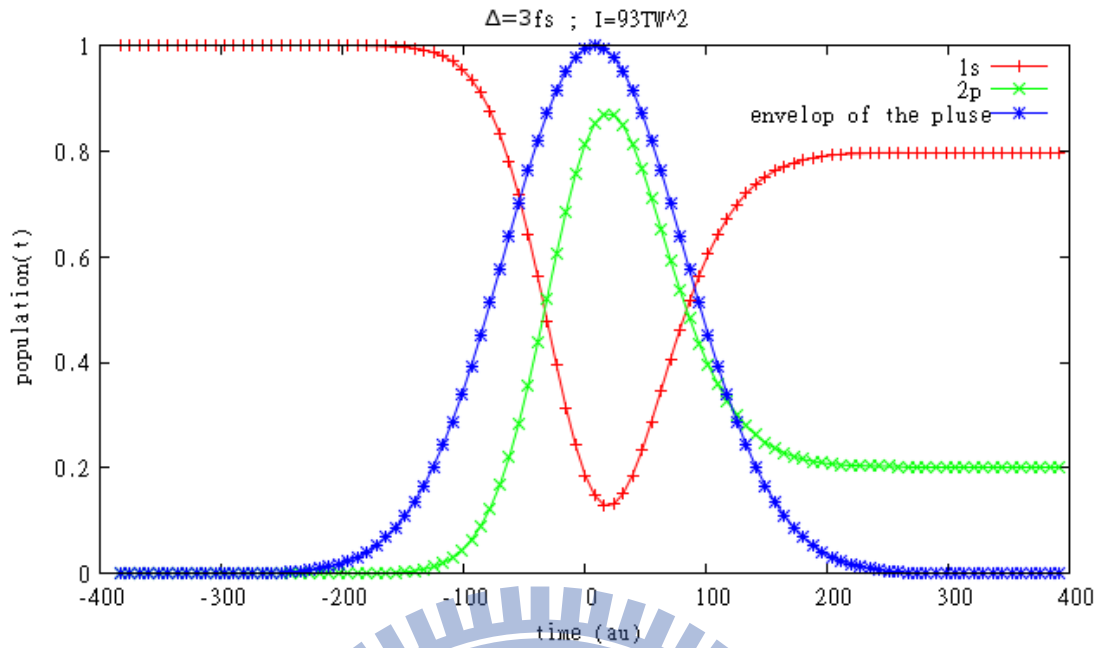


Fig.3-2. The red bar line is hydrogen ground state population history , the green cross line is 2p state population history ,and the blue star line is envelop of the pluse in 3fs FWHM and 93 TW/cm²

Although using different intensity , the result of two state population after fluctuation will be similar

4. Numerov method

For transition amplitudes $M_{p,i}^{(X)}$, and $M_{p,2p}^{(L)}$ need calculate incoming scattering wave $\Psi_p^-(\vec{r})$, here using numerov method to solve. Numerov's method is an efficient algorithm for solving second-order differential equations of the form

$$\frac{d^2y}{dx^2} = U(x) + V(x) \cdot y \quad (4.1)$$

using numerov method can find the relation:

$$\left(1 - \frac{h^2}{12}V_{n+1}\right)y_{n+1} = \left(1 + \frac{5h^2}{12}V_{n+1}\right)2y_n - \left(1 - \frac{h^2}{12}V_{n-1}\right)y_{n-1} + \frac{h^2}{12}(U_{n+1} + 10U_n + U_{n-1}) + O(h^6) \quad (4.2)$$

The continuum wave function $\Psi_k^-(\vec{r})$ then satisfies the Schrödinger equation

$$\left[-\frac{\nabla^2}{2} + V(r) - \frac{k^2}{2}\right] \Psi_k^-(\vec{r}) = 0 \quad (4.3)$$

where the Coulomb potential in hydrogen atom $v(r) = \frac{-1}{r}$ (no short-range v)

The incoming scattering wave can be expanded in terms of partial waves as

$$\Psi_k^-(\vec{r}) = \frac{1}{\sqrt{k}} \sum_{l=0}^{\infty} \sum_{-l}^l i^l e^{-i\sigma_l} R_{El}(r) Y_l^m(\Omega_r) Y_l^{m*}(\Omega_k) \quad (4.4)$$

here σ_l is the Coulomb phase shift

$$\gamma = -\frac{z}{k}; \sigma_l = \arg\Gamma(l + 1 + i\gamma) \quad (4.5)$$

with the asymptotic nuclear charge $z=1$. R_{El} is the energy normalized radial wave function such that

$$\int_0^{\infty} R_{E'l}(r)R_{E'l'}(r) r^2 dr = \delta(E - E') \quad (4.6)$$

and has the asymptotic form

$$R_{E'l}(r) \xrightarrow{\infty} \frac{1}{r} \sqrt{\frac{2}{\pi k}} \sin \left[kr - \frac{l\pi}{2} - \gamma \ln(2kr) + \sigma_l \right] \quad (4.7)$$

$$\frac{d^2 y}{dx^2} u_l(r) = \left[\frac{l(l+1)}{r^2} + \frac{2mv(r)}{\hbar^2} - k^2 \right] u_l(r) \quad (4.8)$$

For the Coulomb project consider the hydrogen atom

$$\Psi(r) = \frac{u_l(r)}{r} Y_l^m(\theta, \phi) \quad (4.9)$$

$$V(r) = -\frac{1}{r} \quad E = \frac{\hbar^2 k^2}{2m} \quad (4.10)$$

$$\Rightarrow \frac{d^2 u_l(r)}{dx^2} = \left[\frac{l(l+1)}{r^2} + \frac{2}{r} - 2E \right] u_l(r) \quad (4.11)$$

$$u_l(r=0) = 0$$

$$u_l(r=h) = he^{-\frac{h^2}{2}} \quad (4.12)$$

the numerical result in Fig.4-1. ,Fig.4-2. .

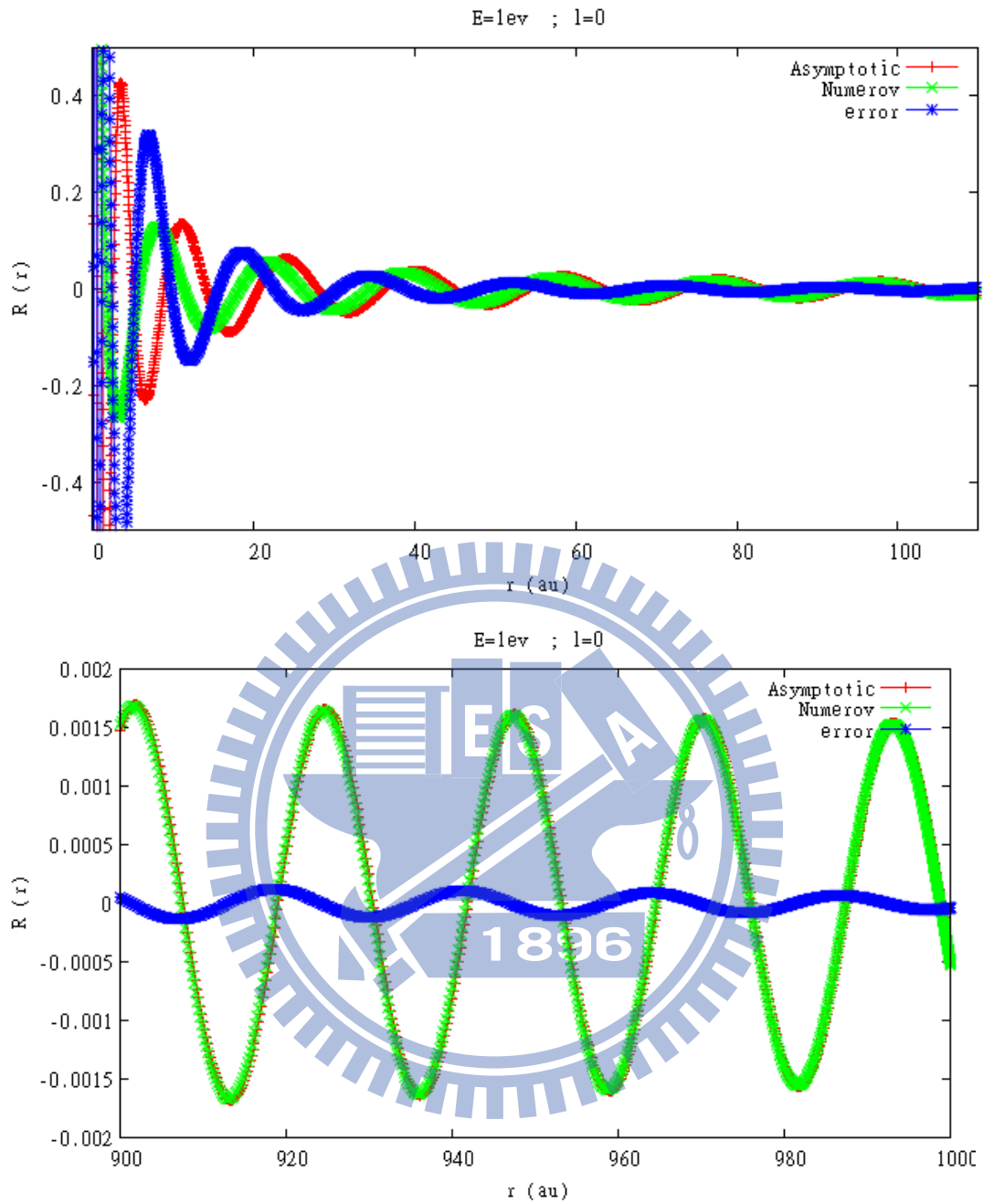


Fig.4-1. Compare asymptotic form and Numerov method in 1ev $l=0$. The Red bar line is using asymptotic form , green cross line is using numerov method , and blue star line is error of Numerov minus asymptotic.

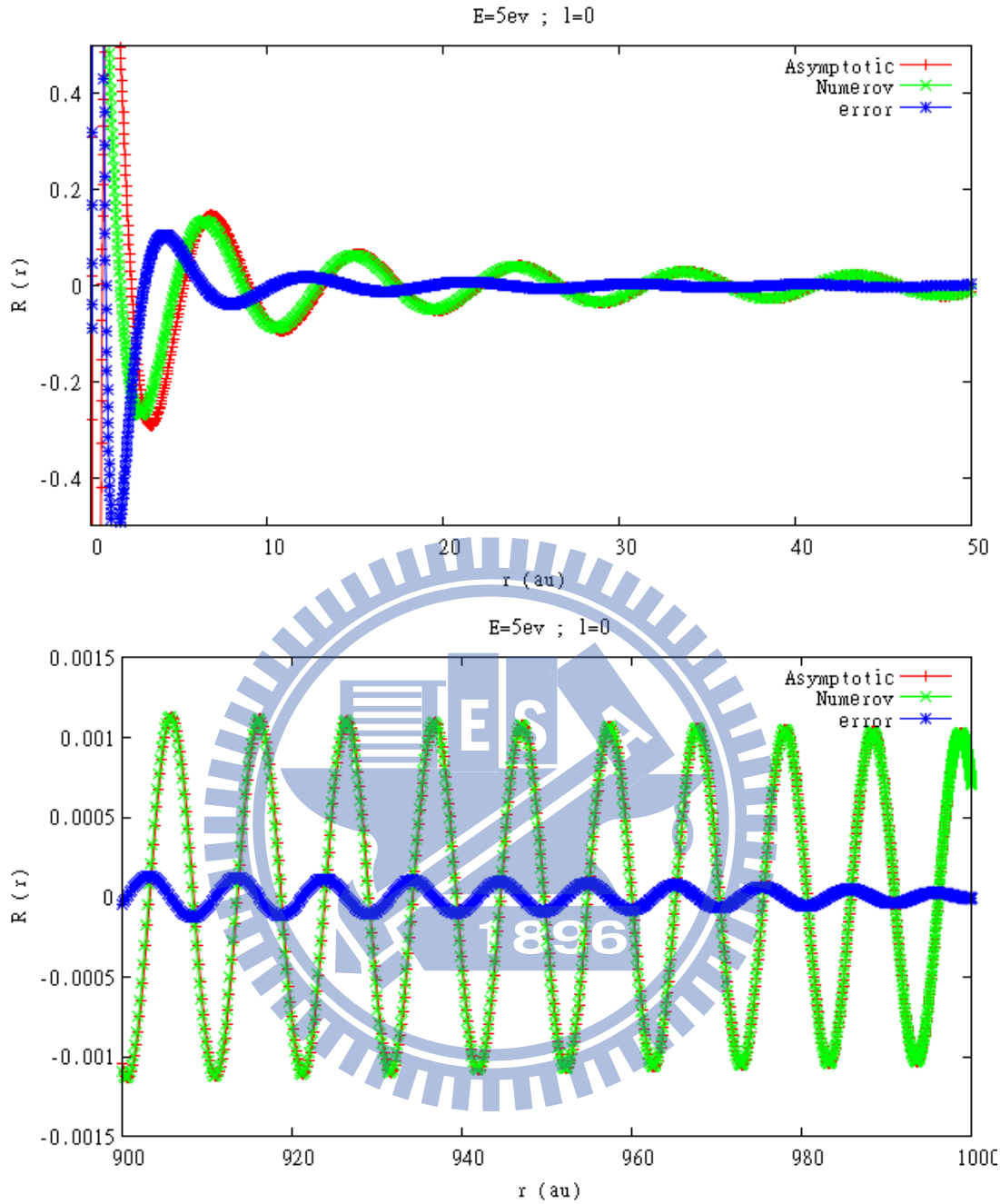


Fig.4-2. Compare asymptotic form and Numerov method in 5ev $l=0$. The Red bar line is using asymptotic form , green cross line is using numerov method , and blue star line is error of Numerov minus asymptotic.

Form Fig.4-1. and Fig.4-2. can find when use higher E the numerov method will quick match asymptotic form in r .

5. First order time-depended perturbation to continuum

The ionization amplitudes of the pump pulse can be solved by first-order perturbation theory. The transition amplitude to the continuum states is calculated from Quantum Physics textbook :

$$M_{\mathbf{p},i}^{(X)} = -i \int_{-\frac{\tau_X}{2}}^{\frac{\tau_X}{2}} dt e^{-i(\epsilon_{1s} - \epsilon_{\mathbf{p}})(t - \frac{\tau_X}{2})} \langle \Psi_{\mathbf{p}}^-(\vec{r}) | \hat{\epsilon} \cdot \vec{r} E_X(t) | \phi_{1s}(\vec{r}) \rangle \quad (5.1)$$

where the incoming scattering wave $\Psi_{\mathbf{p}}^-$ can be found in Chapter 4.

with the gaussian $E(t) = \hat{\epsilon} E_m \cdot e^{-\frac{2\ln 2}{\Delta^2} t^2} \cdot \cos(\omega t + \varphi)$ the CEP phase φ can be set to 0 , polarization $\hat{\epsilon}$ is along z-axis , the photoelectron energy is $\epsilon_{\mathbf{p}} = \frac{|\mathbf{p}|^2}{2}$. The ionization probability density is shown in

Fig.2b, which is in good agreement with results from solving the TDSE. For hydrogen from ground state to continuous state of incoming boundary condition, for pulse in $[-\frac{\tau_X}{2}, \frac{\tau_X}{2}]$ then

$$M_{\mathbf{p},i}^{(X)} = -i \int_{-\frac{\tau_X}{2}}^{\frac{\tau_X}{2}} dt e^{-i(\epsilon_{1s} - \epsilon_{\mathbf{p}})(t - \frac{\tau_X}{2})} E(t) \langle \Psi_{\mathbf{p}}^-(\vec{r}) | \hat{\epsilon} \cdot \vec{r} | \phi_{1s}(\vec{r}) \rangle \quad (5.2)$$

keep the slowly varying term

$$\begin{aligned} & \approx -i \int_{-\frac{\tau_X}{2}}^{\frac{\tau_X}{2}} dt e^{-i(\epsilon_{1s} - \epsilon_{\mathbf{p}})(t - \frac{\tau_X}{2})} E_m \cdot e^{-\frac{2\ln 2}{\Delta^2} t^2} \cdot \frac{1}{2} e^{-i\omega t} \langle \Psi_{\mathbf{p}}^-(\mathbf{r}) | \hat{\epsilon} \cdot \mathbf{r} | \phi_{1s}(\mathbf{r}) \rangle \\ & = \frac{(-1)^1 E_m}{2} e^{i[\sigma_1 - \frac{\tau_X}{2}(\epsilon_{\mathbf{p}} - \epsilon_{1s})]} \int_{-\frac{\tau_X}{2}}^{\frac{\tau_X}{2}} dt e^{i(\epsilon_{\mathbf{p}} - \epsilon_{1s} - \omega)t} \cdot e^{-\frac{2\ln 2}{\Delta^2} t^2} \cdot \langle \mathbf{p} | \hat{\epsilon} \cdot \vec{r} | \phi_{1s}(\vec{r}) \rangle \\ & a \equiv \frac{2\ln 2}{\Delta^2} \end{aligned} \quad (5.3)$$

$$= \frac{(-1)^l E_m}{2} e^{i[\sigma_1 - \frac{\tau_X}{2}(\epsilon_p - \epsilon_{1s})]} \cdot \langle \mathbf{p} | \hat{\epsilon} \cdot \vec{r} | \varphi_{1s}(\vec{r}) \rangle \int_{-\frac{\tau_X}{2}}^{\frac{\tau_X}{2}} dt e^{i(\epsilon_p - \epsilon_{1s} - \omega)t} \cdot e^{-at^2} \quad (5.4)$$

$$e^{i(\epsilon_p - \epsilon_{1s} - \omega)t} \cdot e^{-at^2} = \exp\{-[at^2 - i(\epsilon_p - \epsilon_{1s} - \omega)t]\} \quad (5.5)$$

$$= \exp\left\{-\left[at^2 - i(\epsilon_p - \epsilon_{1s} - \omega)t - \frac{(\epsilon_p - \epsilon_{1s} - \omega)^2}{a}\right] + \frac{(\epsilon_p - \epsilon_{1s} - \omega)^2}{a}\right\}$$

$$= \exp\left\{-\left[\sqrt{a}t - \frac{i(\epsilon_p - \epsilon_{1s} - \omega)}{\sqrt{a}}\right]^2 + \frac{(\epsilon_p - \epsilon_{1s} - \omega)^2}{a}\right\} \quad (5.6)$$

$$M_{\mathbf{p},i}^{(X)} = \frac{(-1)^l E_m}{2} e^{i[\sigma_1 - \frac{\tau_X}{2}(\epsilon_p - \epsilon_{1s})]} \cdot \langle \mathbf{p} | \hat{\epsilon} \cdot \vec{r} | \varphi_{1s}(\vec{r}) \rangle \cdot e^{-\frac{(\epsilon_p - \epsilon_{1s} - \omega)^2}{a}} \cdot \sqrt{\frac{\pi}{a}}$$

$$M_{\mathbf{p},i}^{(X)} = (-1)^l e^{i[\sigma_1 - \frac{\tau_X}{2}(\epsilon_p - \epsilon_{1s})]} E_m \sqrt{\frac{\pi \Delta^2}{8 \ln 2}} \cdot e^{-\frac{(\epsilon_p - \epsilon_{1s} - \omega)^2 \Delta^2}{8 \ln 2}} \cdot \langle \mathbf{p} | \hat{\epsilon} \cdot \vec{r} | \varphi_{1s}(\vec{r}) \rangle \quad (5.7)$$

$$\langle \mathbf{p} | \hat{\epsilon} \cdot \vec{r} | \varphi_{1s}(\vec{r}) \rangle = \sum_{l=0}^{\infty} \sum_{m=-l}^l \int R_{E1}^*(r) Y_l^{m*}(\Omega_r) Y_l^m(\Omega_k) \sqrt{\frac{4\pi}{3}} Y_1^0(\vec{r}) \cdot \mathbf{r} \cdot R_{10}(r) Y_0^0 r^2 d\Omega dr \quad (5.8)$$

use $\int Y_l^m Y_l^{m'*} d\Omega = \delta_{ll'} \delta_{mm'}$

$$\langle \mathbf{p} | \hat{\epsilon} \cdot \vec{r} | \varphi_{1s}(\vec{r}) \rangle = \sqrt{\frac{1}{3}} Y_1^0(\Omega_k) \int R_{E0}^*(r) R_{10}(r) \cdot r^3 d\Omega dr$$

$$= \sqrt{\frac{1}{4\pi}} \cos\theta_k \int R_{E0}^*(r) R_{10}(r) \cdot r^3 d\Omega dr \quad (5.9)$$

R_{E0} solve by Numerov method

$M_{\mathbf{p},i}^{(X)}$ real and image term amplitudes and probability density in Fig. 5-1. and Fig. 5-2.

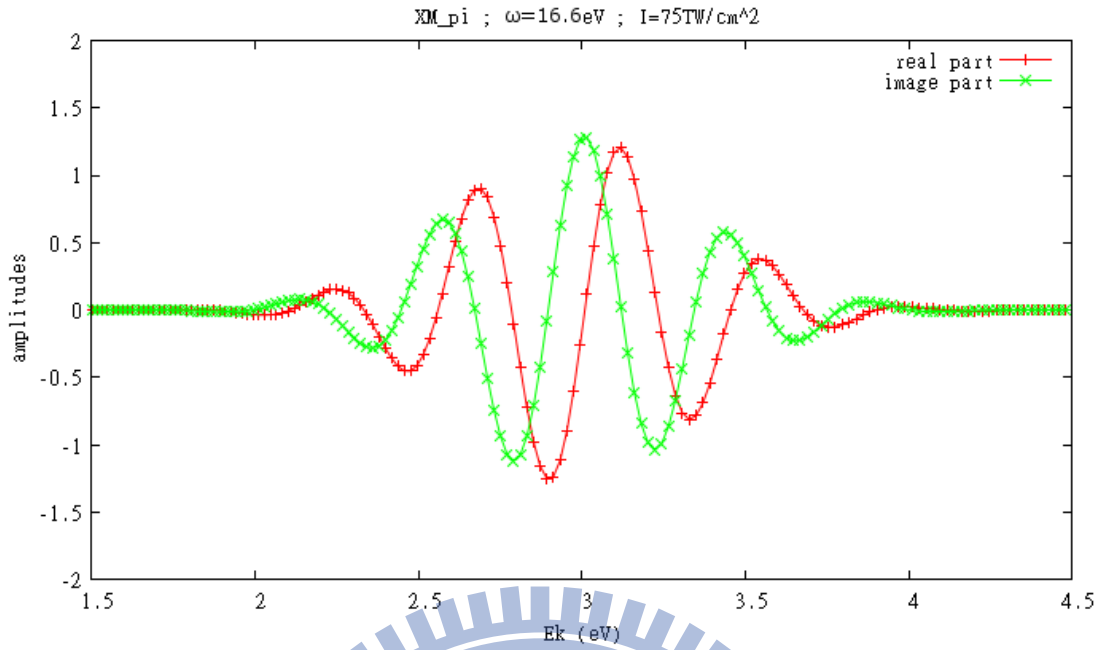


Fig. 5-1. The red bar line is $M_{p,i}^{(X)}$ real term amplitude and green cross is $M_{p,i}^{(X)}$ image term amplitude, 3fs FWHM and 75TW/cm²

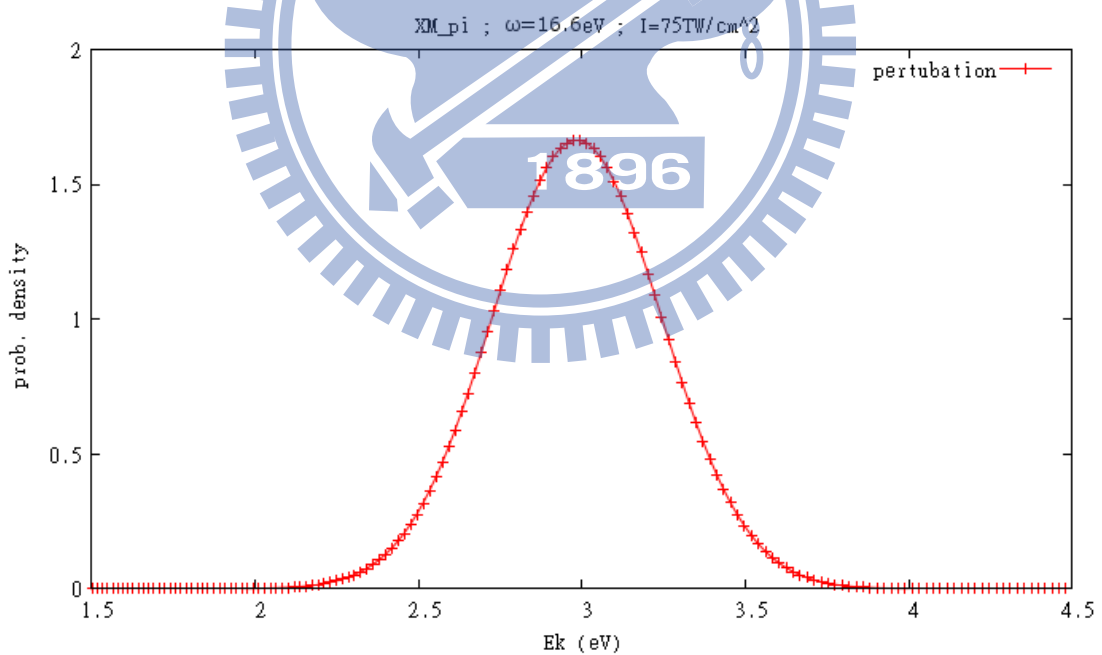


Fig. 5-2. The red bar line is $M_{p,i}^{(X)}$ probability density with photoelectron energy. The laser pulse use 3fs FWHM and 75TW/cm²

With $M_{p,i}^{(X)}$ and $M_{2p,i}^{(X)}$ obtained, the time evolution of the electronic wave packet can be easily obtained. In an experiment, of course the goal is to apply a probe pulse at different time delays from which information about this wave packet can be uncovered. We note that the whole electron wave packet actually includes the contribution from the 1s part. However, the 1s state is energetically well separated from the 2p and the continuum electrons, we can use a low-energy probe pulse without perturbing the 1s part of the wave packet.

For the one-photon absorption by the probe pulse, first-order perturbation theory gives

$$M_{p,2p}^{(L)} = -i \int_{\tau - \frac{\tau_L}{2}}^{\tau + \frac{\tau_L}{2}} dt e^{-i(\epsilon_{2p} - \epsilon_p)[t - (\tau - \frac{\tau_L}{2})]} \langle \Psi_p^-(\vec{r}) | \hat{\epsilon} \cdot \vec{r} E_L(t - \tau) | \phi_{2p}(\vec{r}) \rangle \quad (5.10)$$

$M_{p,2p}^{(L)}$ also with the gaussian $E(t) = \hat{\epsilon} E_m \cdot e^{-\frac{2 \ln 2}{\Delta^2} t^2} \cdot \cos(\omega t + \varphi_p)$ the CEP phase φ_p can be set 0, too. The polarization $\hat{\epsilon}$ is also along z-axis. For hydrogen from ground state to continuous state of incoming boundary condition, for pulse in $[\tau - \frac{\tau_L}{2}, \tau + \frac{\tau_L}{2}]$

Use the same method

$$M_{p,2p}^{(L)} = (-1)^l e^{i[\sigma_1 - \frac{\tau_L}{2}(\epsilon_p - \epsilon_{2p}) + \varphi_p]} E_m \sqrt{\frac{\pi \Delta^2}{8 \ln 2}} \cdot e^{-\frac{(\epsilon_p - \epsilon_{2p} - \omega)^2 \Delta^2}{8 \ln 2}} \cdot \langle \mathbf{p} | \hat{\epsilon} \cdot \vec{r} | \varphi_{2p}(\vec{r}) \rangle \quad (5.11)$$

$$\langle \mathbf{p} | \hat{\epsilon} \cdot \vec{r} | \varphi_{2p}(\vec{r}) \rangle = \sum_{l=0}^{\infty} \sum_{m=-l}^l \int R_{El}^*(r) Y_l^{m*}(\Omega_r) Y_l^m(\Omega_k) \sqrt{\frac{4\pi}{3}} Y_1^0(\vec{r}) \cdot \mathbf{r} \cdot R_{21}(r) Y_1^0(\vec{r}) \cdot r^2 d\Omega dr \quad (5.12)$$

$$Y_1^0(\vec{r}) Y_1^0(\vec{r}) = \frac{3}{4\pi} \cos^2 \theta = \frac{3}{4\pi} \left[\frac{1}{3} (3 \cos^2 \theta - 1) + \frac{1}{3} \right] = \frac{3}{4\pi} \left[\frac{4}{3} \sqrt{\frac{\pi}{5}} Y_2^0 + \frac{\sqrt{4\pi}}{3} Y_0^0 \right] \quad (5.13)$$

$$\begin{aligned}
\langle \mathbf{p} | \hat{\epsilon} \cdot \vec{r} | \varphi_{2p}(\vec{r}) \rangle &= \sqrt{\frac{4}{15}} Y_2^0(\Omega_k) \int R_{E2}^*(r) R_{10}(r) \cdot r^3 d\Omega dr + \sqrt{\frac{1}{4\pi}} Y_0^0(\Omega_k) \int R_{E0}^*(r) R_{10}(r) \cdot r^3 d\Omega dr \\
&= \sqrt{\frac{1}{12\pi}} (3\cos^2 \theta_k - 1) \int R_{E2}^*(r) R_{10}(r) \cdot r^3 d\Omega dr + \frac{1}{4\pi} \int R_{E0}^*(r) R_{10}(r) \cdot r^3 d\Omega dr
\end{aligned}
\tag{5.14}$$

R_{E2} and R_{E0} are also solve by Numerov method.

As well as , $M_{p,2p}^{(L)}$ real and image term amplitudes and probability density in Fig. 5-3. and Fig. 5-4. .

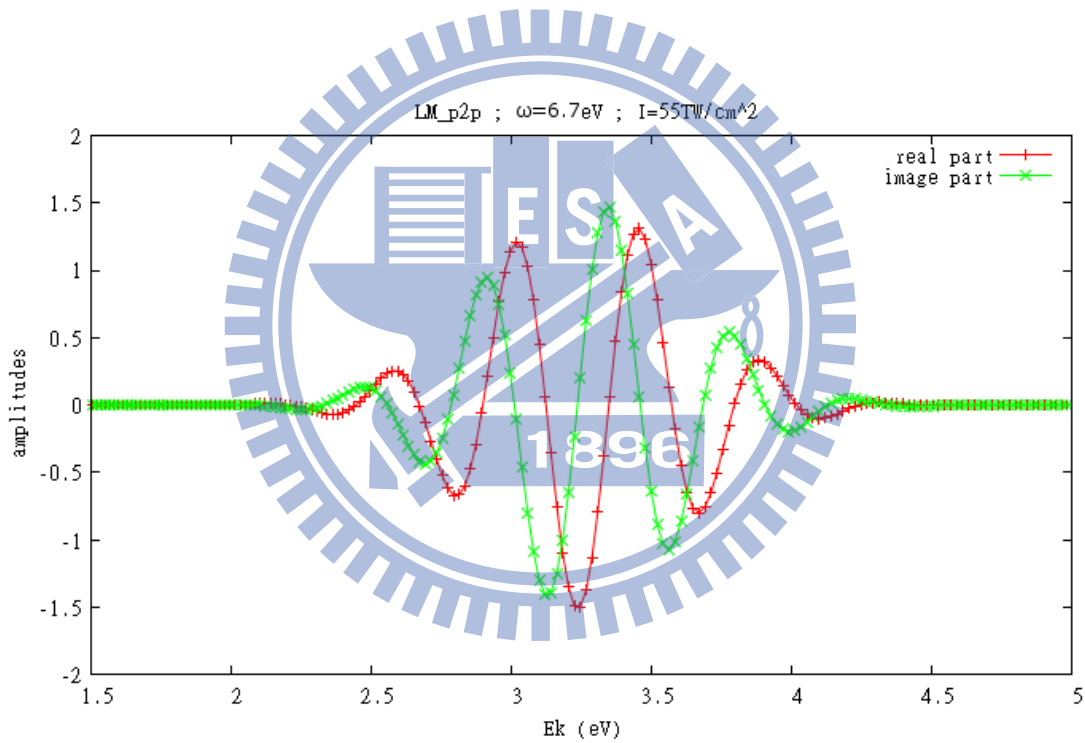


Fig. 5-3. The red bar line is $M_{p,2p}^{(L)}$ real term amplitude and green cross is $M_{p,2p}^{(L)}$ image term amplitude , 3fs FWHM and 55TW/cm²

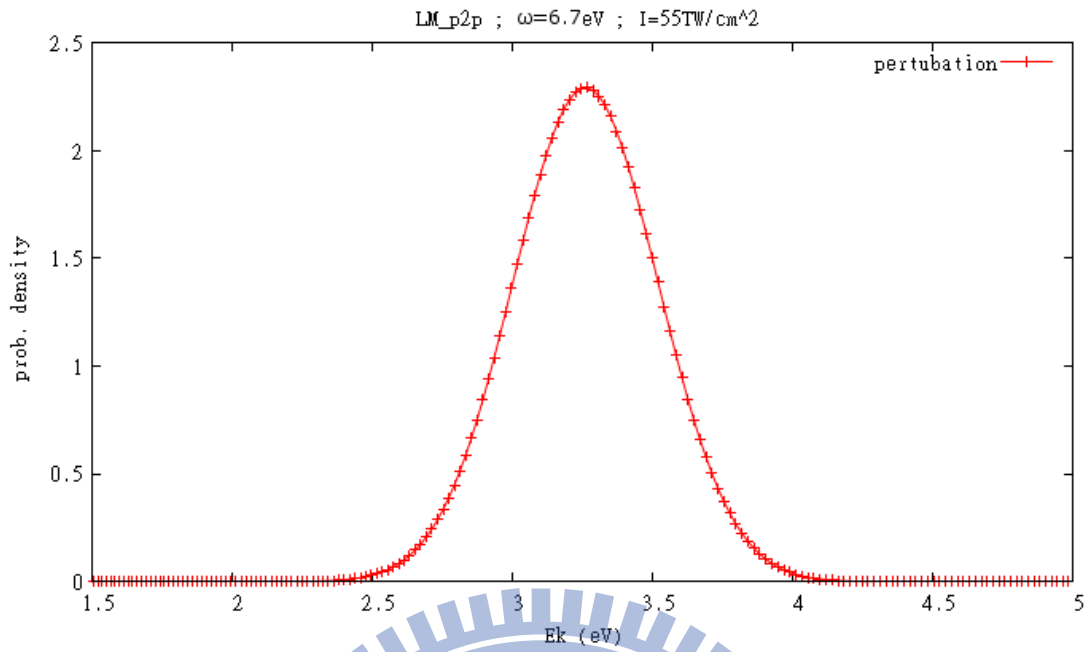
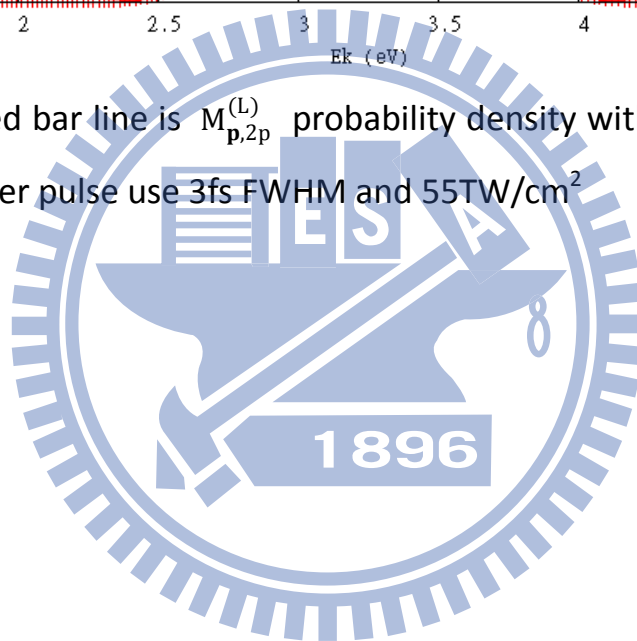


Fig. 5-4. The red bar line is $M_{p,2p}^{(L)}$ probability density with photoelectron energy. The laser pulse use 3fs FWHM and $55\text{TW}/\text{cm}^2$



6. Results

When get the transition amplitudes $M_{p,2p}^{(L)}$, $M_{2p,i}^{(X)}$, and $M_{p,i}^{(X)}$, then combine to find $|M_{pi}(\tau)|^2$ in Fig. 6-1. and Fig. 6-2.

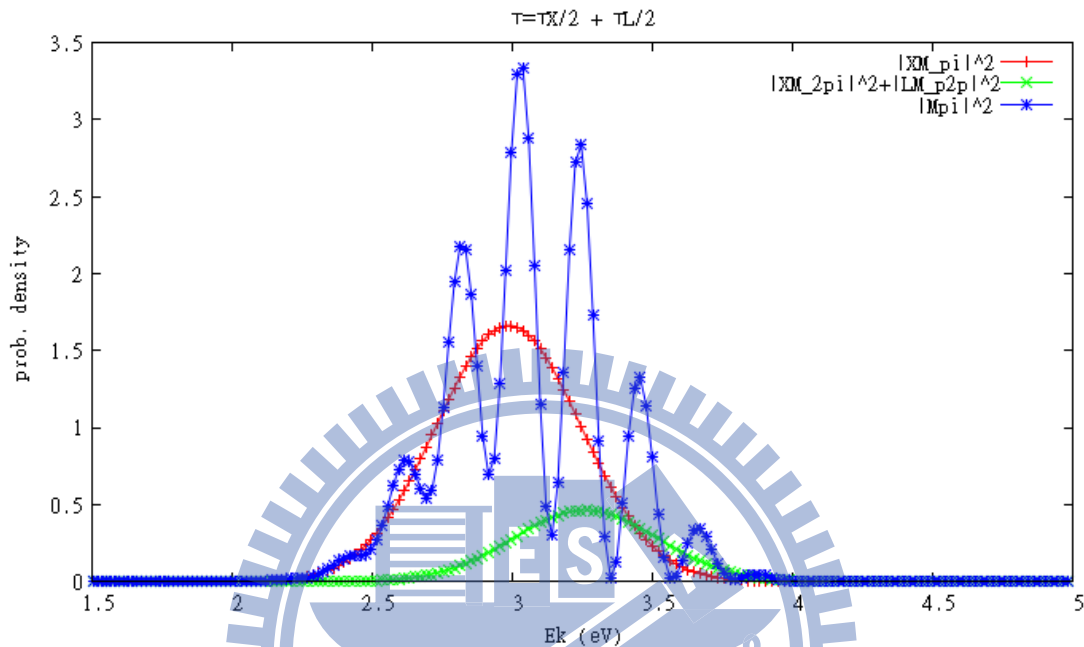


Fig.6-1. Photoelectron energy spectrum $|M_{pi}(\tau)|^2$ (blue star line) obtained by $\theta_k=45^\circ$ and time-delay $\tau = \frac{\tau_L}{2} + \frac{\tau_x}{2}$ with $|M_{p,i}^{(X)}|^2$ (red bar line) and $|M_{2p,i}^{(X)} M_{p,2p}^{(L)}|^2$ (green cross line)

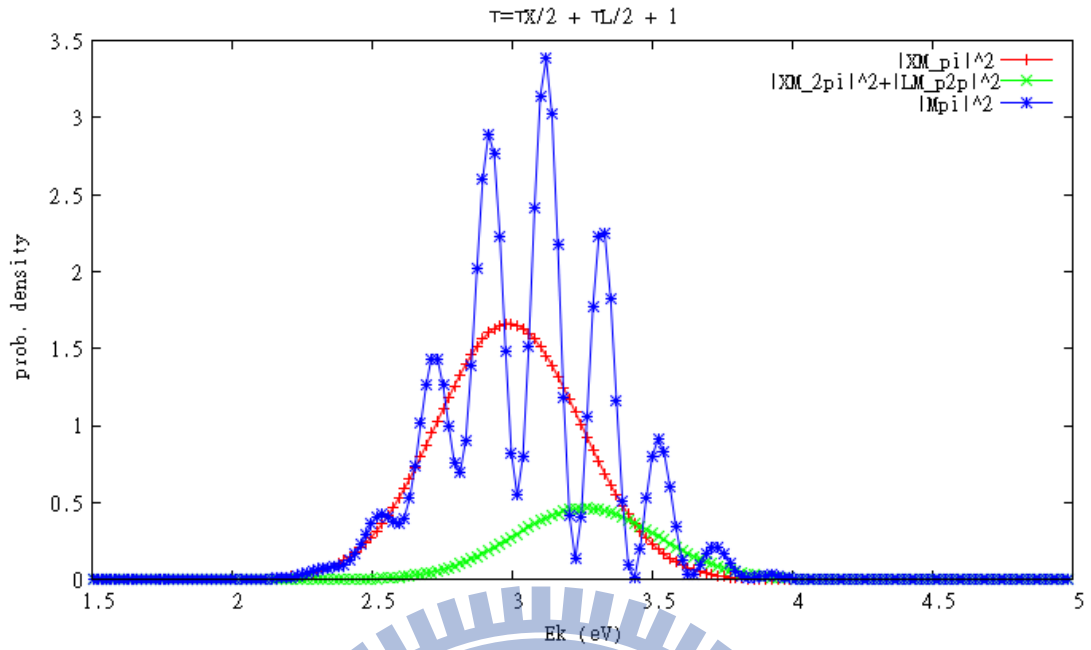


Fig.6-2. Photoelectron energy spectrum $|M_{pi}(\tau)|^2$ (blue star line) obtained by $\theta_k=45^\circ$ and time-delay $\tau = \frac{\tau_L}{2} + \frac{\tau_X}{2} + 1$ with $|M_{p,i}^{(X)}|^2$ (red bar line) and $|M_{2p,i}^{(X)} - M_{p,2p}^{(L)}|^2$ (green cross line)

The interference in the angular distribution in Fig.6-3. can be understood from the angular momentum components of the photoelectrons.

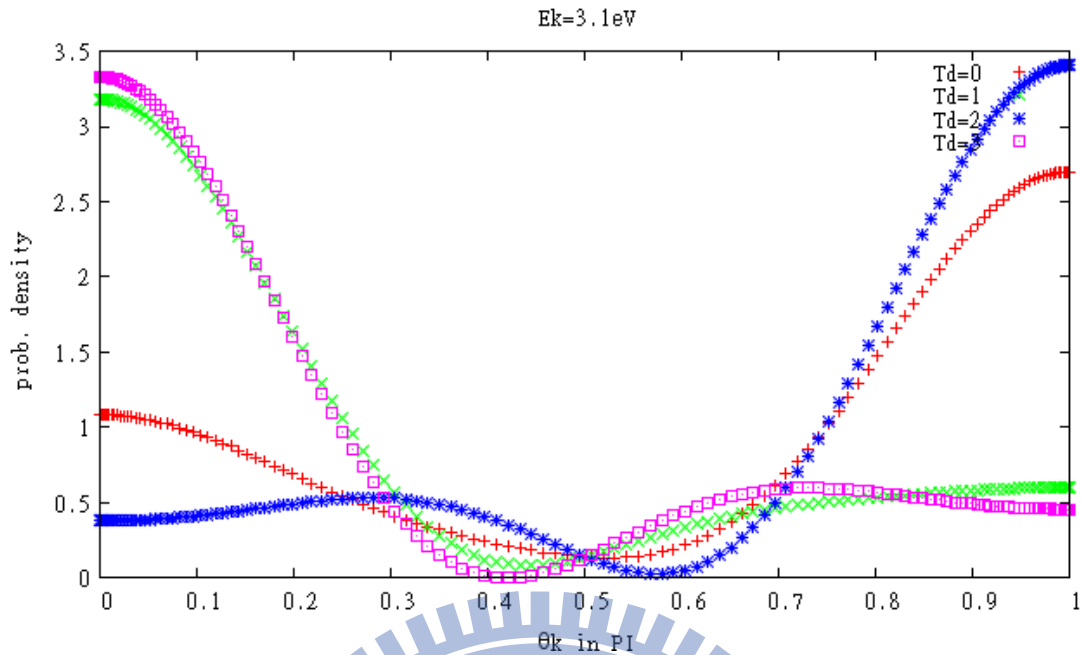


Fig.6-3. Angular distribution of photoelectron for a fixed energy $\epsilon=3.1\text{eV}$

at several delay-times. Here $\tau = \frac{\tau_L}{2} + \frac{\tau_x}{2} + T_d$ so $T_d = \frac{\tau_L}{2} + \frac{\tau_x}{2} + \tau$

For the narrow energy range where the electron yields are large, we can expect all the other parameters are nearly energy independent, thus the peaks of the spectra occur when

$$\Phi_{p,2p} - (\epsilon_p - \epsilon_{2p})\tau = 2n\pi$$

where n is a positive or negative integer. This equation shows that the peak shall follow a hyperbola with the peak shifts to smaller τ for larger ϵ . Thus the hyperbola is tilted toward smaller τ for larger ϵ (and larger τ for smaller ϵ). The tilt is more toward the horizontal axis as τ increases.

These general features can be clearly seen in Fig.6-4. and Fig.6-5.

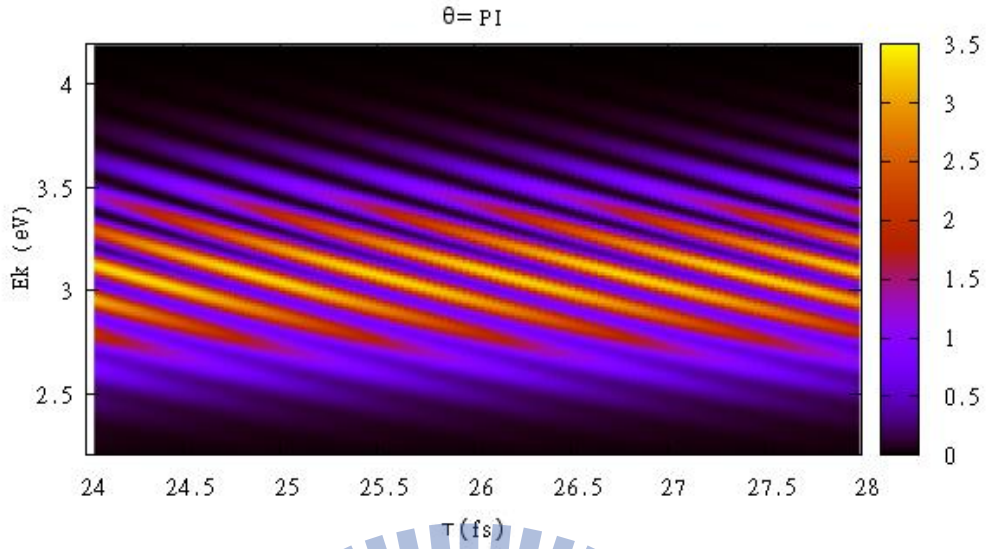


Fig.6-4. Interferogram for $\theta_k = \pi$ depend on time-delay τ .

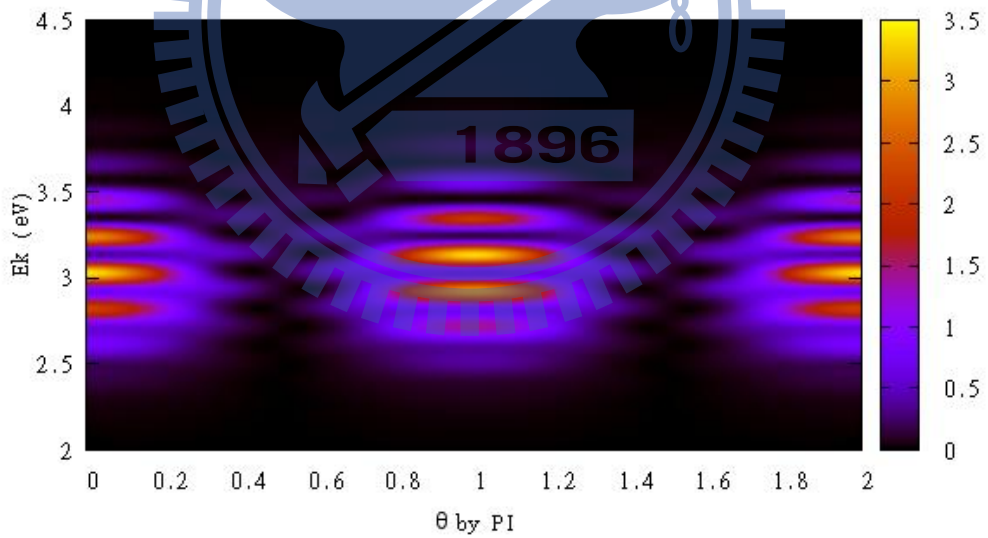


Fig.6-5. Interferogram for fix time-delay $\tau = \frac{\tau_L}{2} + \frac{\tau_x}{2}$ and depend on $\theta_k = [0, 2\pi]$.

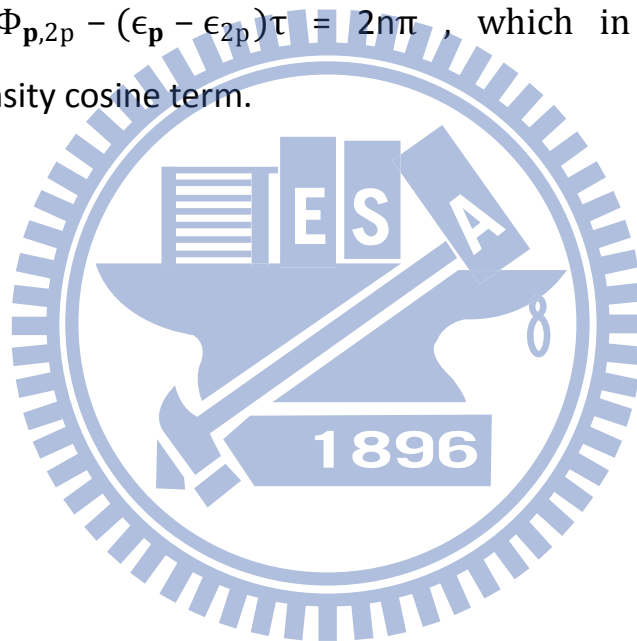
7. Conclusion

The model of pump-probe process using by pump and probe laser.

The pump process combination by two step. First, using laser for bound-bound excitation (from 1s to 2p), and second 1st-order perturbation for bound (2p) to continuum state.

The probe pulse also have two effects. First, the continuous wave packet is Volkov like, time-delay $\tau=0$ with Gaussia pulse. 1s2p + laser calculated by 1st-order perturbation.

The interferogram show by hyperbola and peaks of the spectra occur when $\Phi_{p,2p} - (\epsilon_p - \epsilon_{2p})\tau = 2n\pi$, which in the ionization probability density cosine term.



Reference

- [1] X.M. Tong and C.D. Lin, J. Phys. B38, 2593 (2005).
- [2] See for example, S. Gasiorowicz, Quantum Physics, 2nd ed. Chapter 21 (John-Wiley & Sons, New York,1996).
- [3] Anh-Thu Le,R.R. Lucchese, S. Tonzani, T. Morishita, and C. D. Lin, Phys. Rev.A80, 013401 (2009).
- [4] Louis H. Haber, Benjamin Doughty,and Stephen R.Leone, Phys. Rev. A79,031401R (2009).
- [5] F. Kelkensberg et al., Phys. Rev. Lett. 103, 123005 (2009).
- [6] J. L. M. Quiroz González and D. Thompson
(Received 7 April 1997; accepted 28 May 1997)



Appendix

Atomic units

Atomic units (au) form a system of units convenient for atomic physics, electromagnetism, and quantum electrodynamics, especially when the focus is on the properties of electrons.

In **au**, the numerical values of the following four fundamental physical constants are all unity by definition:

$$\text{Electron mass} \quad : \quad m_e = 1$$

$$\text{Elementary charge} \quad : \quad |e| = 1$$

$$\text{reduced Planck's constant} \quad : \quad \hbar = 1$$

$$(1) \text{ Unit of charge} = \text{charge of electron} = |e| = 1.602 \times 10^{-19} \text{ C}$$

$$(2) \text{ Unit of mass} = \text{mass of electron} = m_e = 9.109 \times 10^{-31} \text{ kg}$$

$$(3) \text{ Unit of length} = \text{radius of ground state}$$

$$= 1 \text{ bohr}$$

$$= 0.53 \times 10^{-10} \text{ m}$$

$$= 0.53 \text{ \AA}$$

$$(4) \text{ Unit of time} = \text{period of ground state electron orbiting}$$

$$= \frac{a}{V_0} = \frac{\hbar^3}{me^4} = 2.42 \times 10^{-17} \text{ s}$$

$$(5) \text{ Unit of velocity} = \text{speed of electron}$$

$$= \frac{e^2}{\hbar} = 2.2 \times 10^8 \text{ cm/s}$$

$$= \alpha c = \frac{c}{137.037}$$

$$(6) \text{ Unit of angular frequency} = \frac{V_0}{a} = 4.1 \times 10^{16} \text{ s}^{-1}$$

$$(7) \text{ Unit of energy} = \frac{e^2}{a} = 1 \text{ Hartree} = 2 \text{ Rydberg} = 27.2 \text{ eV}$$

$$(8) \text{ Unit of electric field} = \frac{|e|}{a^2} = 5.14 \times 10^9 \text{ Volt/cm}$$

$$\alpha: \text{ fine structure constant} = \frac{e^2}{\hbar c} = \frac{1}{137.037}$$

$$c: \text{ speed of light} = 137.037$$

Laser intensity in vacuum

$\langle I \rangle$ = time averaged laser intensity

$$= \frac{c}{4\pi} \langle E^2 \rangle$$

$$= \frac{137.037}{4\pi} \cdot \langle E^2 \rangle$$

$$= 7.0192 \times 10^{16} \cdot \langle E^2 \rangle \text{ W/cm}^2$$

$$E = \sqrt{\frac{I}{7.0192 \times 10^{16}}} \text{ a.u.}$$

$$\begin{aligned} 1 \text{ a.u. (intensity)} &= \frac{1 \text{ Hartree}}{(1 \text{ a.u.time})^2} \\ &= \frac{4.36 \times 10^{-18} \text{ J}}{(2.42 \times 10^{-17} \text{ s})(0.53 \times 10^{-8} \text{ cm})^2} \\ &= 6.44 \times 10^{15} \text{ W/cm}^2 \end{aligned}$$

